JOURNAL OF MOLECULAR SPECTROSCOPY 171, 420–434 (1995)

Intensities of Hot-Band Transitions: HCN Hot Bands

ARTHUR MAKI,*,[1] WOLFGANG QUAPP,† AND STEFAN KLEE‡

*Department of Chemistry, University of Washington, Seattle, Washington 98195; †Mathematisches Institut, Universität Leipzig, Augustus-Platz, D-04109 Leipzig, Germany; and ‡Physikalisch-Chemisches Institut, Justus-Liebig-Universität Giessen, Heinrich-Buff-Ring 58, D-35392 Giessen, Germany

A simple vibrational Hönl–London-type formula for hot-band intensities is tested by measuring the intensities of a number of vibrational transitions, including many hot bands, for HCN. This vibrational intensity formula is based on one- and two-dimensional harmonic oscillator functions and a nonlinear electric dipole function that is expanded in a Taylor series with respect to the normal coordinates. It is shown that, when this formula is included, the observed transition dipoles for the bending hot bands differ by only a few percent from the transition dipoles for the same quantum number changes from the ground state. Infrared absorption intensity measurements are given for the transition dipoles for the transitions $01^{1}0$–$00^{0}0$, $02^{0}0$–$00^{0}0$, $03^{1}0$–$00^{0}0$, $04^{0}0$–$00^{0}0$, $10^{0}0$–$01^{1}0$, $12^{0}0$–$00^{0}0$, and $20^{0}0$–$00^{0}0$ and the accompanying hot bands involving the lower states $v_2 = 1$, 2, and 3. This simple model is limited to well-behaved systems, but would be useful for estimating the intensities of some high-temperature spectra. For HCN the Herman–Wallis constants that are quadratic in J (or m) are shown to be determined principally by the effect of l-type resonance.

INTRODUCTION

A little noted fact of spectroscopy is that the hot bands that accompany a room-temperature spectrum have nearly the same transition dipole as the same transition from the ground state, but with simple numerical multipliers that are the vibrational equivalent of the Hönl–London terms. For the most part these terms have been hidden in rather complicated theoretical papers (*1, 2*), but in a few cases they have been explicitly referenced (*3–5*). The simple form of these multipliers is based on harmonic oscillator functions and only considers the first significant terms in the electric dipole function. Except for Ref. (*5*), the terms for doubly degenerate fundamental modes have not been subjected to careful experimental verification. This paper presents measurements of the intensities of the bands $01^{1}0$–$00^{0}0$, $02^{0}0$–$00^{0}0$, $03^{1}0$–$00^{0}0$, $04^{0}0$–$00^{0}0$, $10^{0}0$–$01^{1}0$, $12^{0}0$–$00^{0}0$, and $20^{0}0$–$00^{0}0$, and their hot bands involving transitions from the ν_2, $2\nu_2$, and $3\nu_2$ vibrational states. We have found that, at least for HCN, the simple intensity formula can be applied to the observed intensities to give a transition dipole that is the same, within a few percent, as that found for the transition from the ground state.

Prior to this work absorption intensity measurements had been made on the bending mode of HCN, ν_2, by Hyde and Hornig (*6*) and later by Kim and King (*7*). The intensities of the $2\nu_2$ band near 1400 cm^{-1}, the $\nu_1-\nu_2$ band near 2600 cm^{-1}, and the $3\nu_2$ band near 2113 cm^{-1} also had been measured by Smith (*8*). The intensities of the remaining bands covered by this paper seem not to have been studied. All of the

[1] E-mail: 74301.1264@compuserve.com.

0022-2852/95 $6.00

previous intensity measurements for these bands were conducted with low-resolution spectrometers and at high pressures to eliminate saturation problems. Consequently, only integrated band intensities had been measured for HCN before now. The hot-band intensities were included in those measurements, but were not individually measured.

This is the second paper reporting the results of extensive infrared measurements that we have made on HCN (*9*). Other papers will report the results of wavenumber analyses of these bands and will also give the results of intensity and wavenumber analyses for other bands of HCN and its isotopomers.

EXPERIMENTAL DETAILS

For the present work, Fourier transform spectra were measured on the Bruker IFS120HR high-resolution spectrometer in Giessen. All of the spectra were measured with resolutions that gave experimentally measured linewidths that are very close to the expected linewidth, when both Doppler broadening and pressure broadening are considered.

The measurements were all made at ambient temperatures which varied between 297 and 299 K, although the variation during the course of a single measurement was no more than ±0.9 K from the average. The effective temperature of each measurement was taken as the average of the temperatures at the beginning and end of each run. The temperature was measured by a thermometer attached to the outside of the absorption cell about halfway between the two end mirrors. Although the temperature was measured with a precision of 0.1 K, we estimate that the accuracy of the effective temperature was more like 0.6 to 1.0 K. An uncertainty of 1 K will cause an uncertainty of 3.5% in the intensity of hot bands from the $3\nu_2$ state at 2100 cm^{-1}.

Except for the measurements in the ν_2 and $2\nu_2$ regions, the absorption cell was a multireflection White-type cell designed and built in the Giessen laboratory by Keppler and Rao (*10*). That absorption cell was made of stainless steel and had a base length of 4 m. It was placed between the parallel exit port of the interferometer and the detector chamber using an optically adapted evacuated transfer optics setup. The ν_2 measurements were made with shorter cells; one measurement was made in a small glass absorption cell with a pathlength of 16.5 cm, another was made in a cell with a length of 27 cm, and the others were made with a glass cell with a pathlength of 300 cm. For the $2\nu_2$ spectra we made use of a commercially available White-type borosilicate glass cell (Infrared Analysis Inc., New York) having a baselength of 0.82 m and volume of about 7 liters. The gold mirrors were adjusted to allow for either 4 passes (giving a pathlength of 3.28 m) or 16 passes (13.12 m). The measurements given in this paper were based on pathlengths that varied between 0.165 and 352 m.

Table I indicates the conditions of each measurement. Some entries in Table I may differ from the conditions given in Ref. (*9*) due to our recalibration for the present work. The uncertainty in the measured lengths of the cells is estimated to be in the range of 0.1% (for the long cells) to 1% (for the short cells). Light sources (globar or tungsten lamp), beamsplitters (Ge:KBr or Si:CaF_2), wedged optical windows (KBr or CaF_2), optical interference filters (typically ~800 cm^{-1} FWHM), and detector devices (Ge:Cu at 4 K or InSb at 77 K) were combined to yield optimum instrumental performance in the different spectral regions.

Some difficulty was experienced with changes in the effective pressure of the HCN gas in the absorption cell due to a combination of outgassing and adsorption by the cell walls. Because the high-pressure runs showed smaller variations during the course

TABLE I

Summary of Experimental Conditions for the Measurements

Run	limits (cm^{-1})	Pressure (Pa)	Pathlength (m)	Temp. (K)	Resolution (cm^{-1})
ZZ	560-960	2.95	0.165	297.7	0.0018
Z	560-960	7.24	0.27	298.6	0.0018
V	560-960	4.39	3.0	297.7	0.0018
U	560-960	18.4	3.0	297.9	0.0018
T	560-960	102.	3.0	298.0	0.0018
AT	1200-1800	167.	13.12	296.7	0.0031
AV	1200-1800	35.5	13.12	296.4	0.0031
AX	1200-1800	218.[a]	13.12	297.2	0.0028
AY	1200-1800	117.	3.28	297.2	0.0028
AZ	1200-1800	31.9	3.28	297.5	0.0028
B	1900-2800	9.69	96.	297.4	0.0029
C	1900-2800	31.24	96.	298.6	0.0029
R	1900-2800	490.	240.	298.8	0.0029
AC	2700-3600	100.	192.	298.0	0.0028
H	3800-4900	500.	240.	298.6	0.0086
I	4600-5600	473.3	240.	299.2	0.0098
K	4600-5600	13.2	240.	299.2	0.0098
Q	4600-5600	4.59	240.	298.2	0.0097
AI	5900-7250	205.2	160.	298.0	0.0128
AJ	5900-7250	251.1	352.	297.6	0.0128
AK	5900-7250	21.24	352.	297.2	0.0128
S	5550-6790	233.3	240.	299.1	0.0119

[a] Runs AX, AY, and AZ contained ~95% $H^{12}C^{15}N$ or 4.9% $H^{12}C^{14}N$.

of the measurements, the absolute intensity was estimated from the high-pressure runs, in most cases. The pressure in the absorption cell was measured by two capacitance gauges (MKS baratron, full scale 10 mbar). The accuracy of the pressure gauges is specified to be better than 0.5% of the reading. For each spectral region, the low-pressure measurements were calibrated by using lines from the high-pressure runs to estimate the pressure in the low-pressure runs. This estimate of the pressure was in agreement with the measured pressure, but was more accurate. Because of slow changes in the sample pressure during the course of a measurement, the absolute intensity may be in error by 15% or more but the relative intensity measurements of the ratios of the hot-band intensities divided by the ground state transition intensities are probably accurate to within 5%.

Several different gas samples were used in these measurements. Each sample was purified by repeated vacuum distillation. With the exception of Runs AX, AY, and AZ the samples contained the natural isotopic abundance which may have been slightly different from the abundance given in Table II, simply because of the natural variation of the isotopes or small enrichment effects from different chemical and physical treatments.

THEORY

The integrated absorption intensities (S_i) of individual rovibrational transitions are given by the equations

$$S_i = (1/pl)\int_{+\infty}^{-\infty} \ln(I_0/I)_\nu d\nu$$

$$= (8\pi^3/3hc)\mathcal{L}\nu_i(273.15/T)N_i(C/Q_vQ_R)\mu_v^2F_iS_vS_R \qquad (1)$$

and

$$C = \exp(-E''/kT)\,[1 - \exp(-h\nu_i/kT)], \tag{2}$$

where $\mathcal{L}$ is the Loschmidt constant (2.686763×10^{25} molecules/m^3), T is the temperature (Kelvin), ν_i is the wavenumber (or frequency) of the ith rovibrational transition, p and l are the pressure and pathlength of the sample, respectively, Q_v and Q_R are the vibrational and rotational partition functions respectively, S_v and S_R are the vibrational and rotational intensity factors (S_R is usually called the Hönl–London term), F_i is a function containing the Herman–Wallis correction terms for the rotational dependence of the intensity, μ_i is the transition dipole or dipole derivative for the transition (given in this paper in units of debye), and N_i is the isotopic abundance for the sample. In Eq. (1) we have included the isotopic abundance because the pressure is usually given in terms of the total pressure of the sample rather than the partial pressure of a given isotopic species.

There have been a number of different expressions proposed for the Herman–Wallis function. In this paper, we have followed the lead of Johns and Vander Auwera (*11*) and Watson (*12*) and adopted the expression

$$F^Q = \{1 + A_2^Q J(J+1) + A_4^Q [J(J+1)]^2\}^2 \tag{3}$$

for the Q-branch transitions and

$$F^{PR} = \{1 + A_1^{PR} m + A_2^{PR} m^2 + A_3^{PR} m^3\}^2 \tag{4}$$

for the P- and R-branch transitions. Here m has the usual meaning of $-J''$ for P-branch transitions and $J'' + 1$ for the R-branch transitions. Since F is given as the square of a real function, it can never assume negative values although it can go through zero at some value of m or J.

The Hönl–London terms for $\Delta l = 0$ transitions are given by

$$S_R = (m^2 - l^2)/|m|$$

for P- and R-branch transitions and

$$S_R = (2J+1)l^2/[J(J+1)]$$

for Q-branch transitions. For $\Delta l = \pm 1$ transitions, they are given by

$$S_R = \tfrac{1}{2}(|m| - l\Delta l - 1)(|m| - l\Delta l)/|m|$$

for P-branch transitions,

$$S_R = \tfrac{1}{2}(|m| + l\Delta l + 1)(|m| + l\Delta l)/|m|$$

for R-branch transitions, and

$$S_R = \tfrac{1}{2}(J + l\Delta l + 1)(J - l\Delta l)(2J+1)/[J(J+1)]$$

TABLE II

Parameters Used in the Present Analysis

Percent Isotopic abundance for $^1H^{12}C^{14}N$ = 0.98523 Q_v(298 K) = 1.0676				
for $v_1v_2v_3$ =	000	010	020	030
Q_R(298 K) =	140.45	140.11	139.81	139.54

for Q-branch transitions. For the above equations l is always l'', and $\Delta l = l' - l''$.

The one term in Eq. (1) that is usually omitted is the S_v term because it has the value 1 for transitions from the ground state. However, for hot bands, it is important to include the S_v term. Our S_v term is roughly equivalent to the N_v^2 term of Weber *et al.* (*5*). For those not familiar with this term, a short derivation for nondegenerate vibrations is given in Appendix A. Since the form of the contribution to S_v is different for nondegenerate vibrational modes and for doubly degenerate modes, one can write it as the product of two terms, L_{13} for the nondegenerate vibrations (ν_1 and ν_3) and L_2 for the degenerate vibrational mode (ν_2).

We then have for a linear triatomic molecule such as HCN

$$S_v = L_{13}L_2$$

where

$$L_{13} = (v_1 + \Delta v_1)!(v_3 + \Delta v_3)!/(v_1!v_3!\Delta v_1!\Delta v_3!) \tag{5}$$

with both v_1 and v_3 taking the smaller of the upper and lower state values.

The L_2 term takes a different form according to whether Δv_2 is even or odd. When Δv_2 is even (parallel bands),

$$L_2 = [\tfrac{1}{2}(v_2 + l + \Delta v_2)]![\tfrac{1}{2}(v_2 - l + \Delta v_2)]!/ \{[\tfrac{1}{2}(v_2 + l)]![\tfrac{1}{2}(v_2 - l)]![\tfrac{1}{2}(\Delta v_2)]!^2\} \tag{6}$$

where Δv_2 is always positive and v_2 is the smaller of v_2' or v_2''. When Δv_2 is odd (perpendicular bands),

$$L_2 = [\tfrac{1}{2}(v_2 + l + \Delta v_2 - 1)]![\tfrac{1}{2}(v_2 - l + \Delta v_2 - 1)]![v_2 + l\Delta l + \Delta v_2 + 1]/ \{g_v[\tfrac{1}{2}(v_2 + l)]![\tfrac{1}{2}(v_2 - l)]![\tfrac{1}{2}(\Delta v_2 - 1)]!^2[\Delta v_2 + 1]\}, \tag{7}$$

where Δv_2 is always positive, v_2 is the smaller of v_2' and v_2'', and $g_v = 2$ except that $g_v = 1$ if either l' or l'' is 0. If $v_2 = v_2'$, then $l = l'$ and $\Delta l = l'' - l'$, otherwise $l = l''$ and $\Delta l = l' - l''$.

The g_v term is only needed for calculating rovibrational intensities. It takes into account the restriction that, when one l is zero, only one set of transitions to or from a given vibrational level is allowed, either a Q branch (if the other level is an f level) or else P and R branches (if the other level is an e level), and two sets of transitions are allowed for all other cases. The sum of the line intensities is given by Eq. (7) with the g_v term removed. The g_v term is not needed in the absence of strong Q-branch transitions, i.e., for parallel bands (when Δv_2 is an even integer). Some workers might prefer to include the g_v in the Hönl–London term, S_R, as was done in Ref. (*4*).

ANALYSIS OF THE DATA

The intensity of each rovibrational line was determined by making a nonlinear least-squares fit of the line profile. Figure 1 shows an example of a typical line with the deviations from a least-squares fit indicated as a dashed line. Two different computer programs were used to determine the line intensities: one was a new version of the program used to measure the intensities and linewidths of NO (*13*), and the other was a program developed by Johns and used extensively in his intensity measurements on CO_2 (*11, 14*), among other studies. Both programs gave nearly identical results on those lines where a comparison was made, which includes most of the lines of the

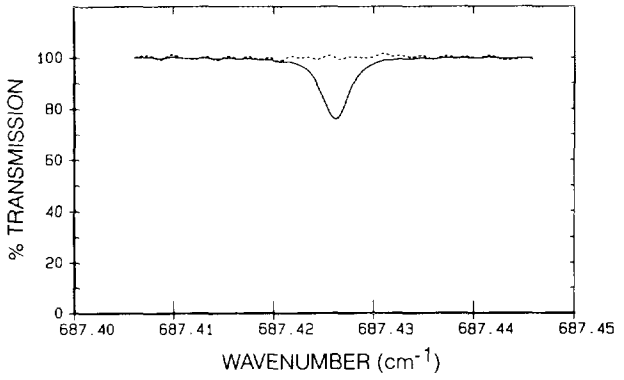

FIG. 1 An. example of the fit of the line profile for the $Q(6)$ line of the $03^{1}0$–$02^{2e}0$ transition of HCN. The solid line indicates the observed intensity and the dashed line indicates the observed minus calculated intensity. Note that the intensity scale for the dashed line is three times the scale for the solid line.

ν_2 and $3\nu_2$ band systems. After comparing the two programs to make certain that they agreed, the program by Johns was preferred because of the many convenient features that it offered, including a more accurate allowance for the instrumental lineshape function for Fourier transform spectra.

Most of the measurements reported here were made on spectra for which the transmission at the peak of the absorption line was greater than 30%. If the peak absorption is too great, the intensity measurement is more sensitive to systematic errors in locating the zero percent transmission line. Such errors are very hard to estimate in FTS spectra. Of course, very weak lines have a smaller signal-to-noise ratio, but that source of error is easy to estimate from the least-squares fit of the line profile.

Another hidden source of error is the occasional coincidence of other lines with the line being measured. Whenever a line was found to be too strong by more than the estimated error, judged by the fit of the other lines, the intensity of that line was given a weight of zero in the least-squares fit used to determine the band intensity and the Herman–Wallis constants. In most cases it was possible to identify an interfering transition. Such overlaps could only cause a line to appear to be too strong; unusually weak lines were retained in the fit as they were assumed to be within the range of experimental error. Whenever nearby transitions might affect the measurement of a given line, those transitions were included in the least-squares fit of the spectrum, provided they were not too strong or too close to the line of interest. Lines were not measured if they were too near to other transitions.

For lines that are pressure broadened, a rather high percentage of the intensity is in the wings of the line and is rather difficult to measure. For that reason, it is important to fit the lineshape to a Voigt profile with the correct pressure-broadened width. The present measurements take the lineshape into account and also make an allowance for the small amount of instrumental distortion of the measured lineshape. Other things, such as signal-to-noise, being equal, the most accurate measurements are those made at pressures below 100 Pa because the lineshape is close to a Gaussian shape which has minimal intensity in the wings. The lower-pressure measurements also avoid the possibility of complications arising from collisional narrowing which was not included in the lineshape analysis.

Many of the measurements were made at pressures low enough to ignore the pressure broadening, nevertheless the effect of pressure broadening was estimated for all the

measurements by using the self-broadening parameters given by Pine and Looney (*15*). When this work was begun, the pressure broadening was determined from the highest pressure measurements, 500 Pa (3.8 Torr), but the measurements of Pine and Looney seem to be more accurate, after allowing for a difference in the definition of the linewidth.

A few of the spectra had asymmetric lineshapes (notably runs H and I) either because of improper adjustment of the optics or because of errors in the phase correction. In those cases only lines with peak absorbances of less than 50% were used and particular attention was paid to processing each line in the same way and with the same lineshape, depending on the rotational quantum number, J. With these precautions the major effect of asymmetric lineshapes will be to produce errors in the absolute intensity assigned to the transitions. For that reason, we believe that the absolute values of the transition dipoles for the 4600 cm^{-1} region could be in error by 20% or more, even though we believe that the relative transition dipoles, comparing the ground state transitions with the hot bands, are quite accurate.

In addition to affecting the value determined for the transition dipole of the hot bands, as discussed earlier, the uncertainty in the temperature of the measurements will affect the value determined for the quadratic Herman–Wallis constants, A_2. We have shown by trial calculation that as a general rule an uncertainty in the temperature of ± 1 K will result in an uncertainty in the A_2^Q term of $\pm 0.15 \times 10^{-4}$. This magnitude of error due to temperature uncertainty is about equal to the statistically determined uncertainty in most cases. As a general rule one does not expect that the A_1^{PR} terms should be affected by temperature uncertainties, but we have found that for some cases the temperature uncertainty will also affect the A_1^{PR} terms by 0.5×10^{-4}, which is close to the statistically determined uncertainty. To some extent this effect is caused by an uneven distribution of the measurements between the P and R branches. The effect of a temperature error will be different for each band, depending on the distribution of the measurements.

RESULTS

Hot-Band Intensities

Table II gives the values for certain parameters that were used in the calculation of the transition dipoles. The isotopic abundances were taken from Refs. (*16–18*). The vibrational partition function was calculated by summing the Boltzmann population of the vibrational energy levels. The rotational partition functions were calculated by applying the equations given by McDowell (*19*). The different vibrational states have slightly different rotational partition functions because of the small differences in the rotational constants.

Tables III and IV give the results of the present intensity measurements. As shown by the tables, when the L_2 term is included in the analysis, the transition dipoles are nearly the same for all the transitions that involve the same quantum number changes. One can see, however, that there seem to be small changes dependent on the lower state involved. Small changes would not be surprising because the higher terms in the dipole moment expansion have been ignored. On the other hand, it is possible that the apparent differences are experimental artifacts.

The present treatment also ignores the effects of any interactions among different vibrational states. Coriolis interactions should not affect the vibrational transition dipole, but purely vibrational interactions, sometimes called Fermi resonances, will

TABLE III

Vibrational Transition Dipoles and Herman-Wallis Constants for Some Perpendicular Bands of $H^{12}C^{14}N$

Transition $v_1'v_2^{l'}v_3'-v_1''v_2^{l''}v_3''$	ν_0 (cm^{-1})	L_2	$\lvert\mu\rvert$ debye[a]	A_1^{PR} $\times10^4$	A_2^{PR} $\times10^4$	A_2^{Q} $\times10^4$	Calc. A_2^{Q} $\times10^4$
01^10-00^00	711.980	1	0.189(1)[b]	6.73(36)	-0.26(3)	-0.19(2)	-0.00(0)
02^00-01^10	699.434	1	0.183(5)	18.87(19)	4.98(2)	-5.35(2)	-5.30(2)
$02^{2e}0-01^10$	714.550	1	0.189(4)	11.3(3)	-4.83(2)	4.11(2)	3.81(6)
$02^{2f}0-01^10$	714.550	1	0.188(4)	9.17(46)	0.26(3)	0.05(3)	0.00(0)
03^10-02^00	702.037	2	0.190(2)	-4.1(12)	4.20(14)	-2.56(3)	-2.594(4)
$03^{1e}0-02^20$	686.921	0.5	0.188(1)	12.(3)	-7.5(2)	-4.16(18)	-3.67(1)
$03^{1f}0-02^20$	686.921	0.5	0.189(1)	26.1(18)	4.06(15)	5.17(10)	5.25(7)
$03^{3e}0-02^20$	717.231	1.5	0.196(1)	17.3(18)	-0.89(15)	1.36(15)	1.08(1)
$03^{3f}0-02^20$	717.231	1.5	0.197(1)	15.(3)	-1.30(18)	0.90(21)	1.364(8)
04^00-03^10	689.509	2	0.185(3)			-8.2(12)	-7.94(4)
$04^{2e}0-03^10$	704.725	1.5	0.196(5)			6.8(17)	6.7(2)
$04^{2f}0-03^10$	704.725	1.5	0.188(7)			-1.4(26)	-1.186(9)
$04^{4e}0-03^30$	720.021	2	0.201(5)			-2.1(19)	0.852(2)
03^10-00^00	2113.450	1	0.003263(1)	-47.4(2)	0.06(2)	-0.30(4)	-0.23(4)
04^00-01^10	2090.979	2	0.00320(1)			-8.11(22)	-8.19(2)
$04^{2e}0-01^10$	2106.196	1.5	0.00330(2)	-22.0(16)	-9.37(16)	6.92(16)	7.93(29)
$04^{2f}0-01^10$	2106.196	1.5	0.00327(1)	-43.9(20)	0.54(11)	0.08(34)	-0.04(1)
05^10-02^00	2083.701	6	0.00323(2)	-53.(3)	2.3(3)	-2.3(4)	-2.60(2)
$05^{1e}0-02^20$	2068.584	1.5	0.00316(5)	-28.(12)	-3.6(12)	-5.2(7)	-4.62(9)
$05^{1f}0-02^20$	2068.584	1.5	0.00307(4)	-52.(11)	5.8(8)	6.3(23)	2.3(2)
$05^{3e}0-02^20$	2099.143	3	0.00324(3)	-16.(6)	-2.8(5)	2.1(17)	2.04(7)
$05^{3f}0-02^20$	2099.143	3	0.00326(4)	-20.(9)	-2.7(6)	2.9(17)	3.20(6)
10^00-01^10	2599.497	1	0.0226(1)	-40.4(1)	0.66(1)	0.33(1)	0.00(0)
11^10-02^00	2592.749	1	0.0226(1)	-68.3(14)	5.20(12)	-4.74(10)	-5.25(2)
$11^{1e}0-02^20$	2577.632	1	0.0232(1)	-37.8(9)	-4.55(10)	0.64(10)	-0.001(1)
$11^{1f}0-02^20$	2577.632	1	0.0232(1)	-43.1(9)	0.79(8)	4.28(24)	3.35(15)
12^00-03^10	2570.859	2	0.0228(1)	-46.9(8)	2.11(11)	-2.72(11)	-2.692(4)
$12^{2e}0-03^10$	2585.758	0.5	0.0220(1)	-50.7(24)	-7.76(23)	6.31(19)	5.35(6)
$12^{2f}0-03^10$	2585.758	0.5	0.0218(1)	-60.8(27)	4.22(36)	-4.60(30)	-3.58(1)
$12^{2e}0-03^30$	2555.447	1.5	0.0233(2)	-80.(10)	-3.1(6)	1.7(20)	1.33(1)
$12^{2f}0-03^30$	2555.447	1.5	0.0236(2)	-57.(7)	-2.3(5)	0.6(16)	1.09(2)

[a] 1 debye = $3.335\,64\times10^{-30}$ C m.

[b] The uncertainty in the last digits is given in parentheses. The uncertainty was determined from a least squares fit of the individual line intensities in a given band and do not reflect absolute uncertainties in the intensities.

clearly have an effect on the intensity through a mixing of the vibrational states. Such vibrational mixing will be different for the levels involved in the hot-band transitions. HCN was chosen for this study because its vibrational states can be fairly well described without invoking the strong Fermi resonance that plagues so many simple molecules such as CO_2. It is quite clear that Eqs. (6) and (7) can not be applied to CO_2 or N_2O unless the effects of Fermi resonance are taken into account.

Herman–Wallis Constants

Tables III and IV also give the Herman–Wallis terms for the different transitions. For the vibrationally degenerate levels that are split into *e* and *f* levels, the vibrational transition dipole is expected to be the same, while the Herman–Wallis constants will generally be different because the *l*-type resonance will redistribute the intensity of the high-*J* rotational transitions and will affect the *e* and *f* levels differently. This was shown in earlier work on HCN (*20*) and Watson has given expressions for the con-

TABLE IV

Vibrational Transition Dipoles and Herman–Wallis Constants for Some Parallel Bands of $H^{12}C^{14}N$

Transition $v_1'v_2^{l'}v_3'$-$v_1''v_2^{l''}v_3''$	ν_0 (cm^{-1})	L_2	$\lvert\mu\rvert$ debye[a]	A_1^{PR} $\times10^4$	A_2^{PR} $\times10^4$	A_2^{Q} $\times10^4$
02^00-00^00	1411.413	1	0.0496(2)[b]	-18.3(10)	0.1(1)	
$03^{1e}0-01^10$	1401.471	2	0.0471(2)	-12.7(8)	0.40(7)	13.4(10)
$03^{1f}0-01^10$	1401.471	2	0.0475(4)	-26.2(11)	0.33(11)	-5.2(9)
04^00-02^00	1391.555	4	0.0489(2)	-20.5(8)	-0.36(8)	
$04^{2e}0-02^20$	1391.646	3	0.0486(2)	-23.6(13)	0.36(10)	
$04^{2f}0-02^20$	1391.646	3	0.0488(2)	-21.4(10)	-0.01(11)	
04^00-00^00	2802.959	1	0.000570(5)	-323.(16)	[0.0]	
$05^{1e}0-01^10$	2783.135	3	0.000561(2)	-87.(8)[c]	[0.0]	
$05^{1f}0-01^10$	2783.135	3	0.000565(3)	-81.(4)	[0.0]	
12^00-00^00	4684.310	1	0.000795(5)	87.6(11)	-0.80(9)	
$13^{1e}0-01^10$	4654.893	2	0.000784(3)	98.5(15)	-1.33(11)	
$13^{1f}0-01^10$	4654.893	2	0.000786(4)	74.9(17)	-1.35(13)	
14^00-02^00	4625.549	4	0.000788(7)	96.9(74)	-2.1(7)	
$14^{2e}0-02^20$	4625.381	3	0.000781(12)	85.9(68)	-1.4(9)	
20^00-00^00	6519.610	1	0.00881(12)	-4.8(4)	0.73(13)	
$21^{1e}0-01^10$	6480.784	1	0.00889(4)	-4.1(6)	0.68(8)	3.8(6)
$21^{1f}0-01^10$	6480.784	1	0.00901(4)	-5.2(4)	0.45(6)	0.9(5)
22^00-02^00	6441.535	1	0.00892(14)	-4.5(20)	-0.09(18)	
$22^{2e}0-02^20$	6442.097	1	0.00886(15)	-3.9(12)	0.45(12)	
$22^{2f}0-02^20$	6442.097	1	0.00888(12)	-2.8(9)	0.22(9)	
20^01-00^01	6488.736	1	0.0087(3)	[-4.0][d]	[0.0]	

[a] 1 debye = $3.335\,64\times10^{-30}$ C m.

[b] The uncertainty in the last digits is given in parentheses. The uncertainty was determined from a least squares fit of the individual line intensities in a given band and do not reflect absolute uncertainties in the intensities.

[c] For $05^{1e}0-01^{1e}0$, $A_3^{PR} = -2.7\pm0.3\times10^{-5}$ was needed in order to allow for the effect of resonance with $2\nu_2+\nu_3$.

[d] Values enclosed in square brackets were fixed.

tributions of l-type resonance to the Herman–Wallis terms (*21*). Figure 2 shows a plot of the measured transition dipole for the 11^10-02^00 and 11^10-02^20 transitions when the Herman–Wallis term is left out. Alternatively one could consider the y-axis to represent the combined term $|\mu F^{1/2}|$.

Maki *et al.* (*20*) showed that l-type resonance causes the high-J transitions of the P and R branch of $02^01-01^{1e}0$ to be stronger than the high-J transitions of the P and R branch of $02^{2e}1-01^{1e}0$, whereas the P- and R-branch transitions of $02^{2f}1-01^{1f}0$ are unaffected. The Q-branch transitions show just the opposite effect. The same principle applies to the 020–010 transitions shown in Fig. 3 as well as the 110–020 transitions shown in Fig. 2.

Watson (*21*) has given a simpler formula for characterizing this effect. When the Fermi resonant terms are eliminated from Watson's formula, one has for 02^00-01^10 $A_2^Q = -A_2^{PR} = -q/\Delta$, where q is the normal l-type resonance constant (0.007483 cm^{-1}) and Δ is the separation of the 02^20 and 02^00 states (15.116 cm^{-1}). The same numbers but with opposite sign apply to the $02^{2e}0-01^10$ transitions. Watson's formula predicts that the quadratic Herman–Wallis constant will be 0.000495 with the appropriate sign. This is very close to the values given in Table III. The same arguments with the same signs will apply to the 11^10-02^00 and $11^10-02^{2e}0$ transitions. In both these cases one would have expected the Herman–Wallis quadratic terms to be zero for the transitions involving the $02^{2f}0$ state. To the extent that those terms

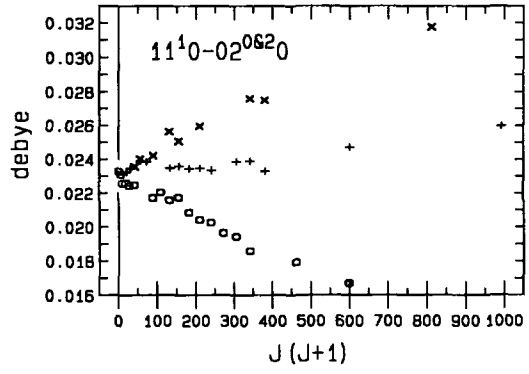

FIG. 2. The transition dipole for the $11^{1e}0$–02^00 transitions (O), for the $11^{1e}0$–$02^{2e}0$ transitions (×), and for the $11^{1f}0$–$02^{2f}0$ transitions (+) as determined by applying Eq. (1) with F_i fixed at the value 1.0; that is to say, no Herman–Wallis constants were applied to the data.

are not zero, they must represent some other effect that probably will also apply to the $02^{2e}0$ state.

In both of the examples cited above the sum of the A_2^{PR} terms does not equal zero, but rather comes close to the value found for the A_2^{PR} term for transitions involving the $02^{2f}0$ state. This residual contribution to the Herman–Wallis constant must come from some other interaction, most likely a Coriolis interaction with more distant energy levels.

The situation is slightly more complicated for the transitions involving the 04^00 and 04^20 states because the l-type resonance also involves the third state, 04^40, although that state is more distant and therefore it affects the other two states only weakly. As a first approximation one can apply Watson's formula to get $A_2^Q = -A_2^{PR} = -q/\Delta = -0.00105$ (for 04^00–01^10) because the effective value for the l-type resonance constant, q, is twice as large for $4\nu_2$. Another complication that affects our ability to measure the transition dipole and Herman–Wallis constants for transitions involving the 04^00 level is the Coriolis interaction with the 01^11 state as described by Maki *et al.* (*20*).

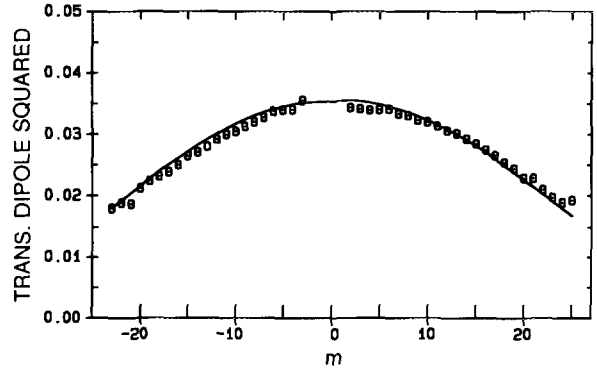

FIG. 3. Square of the transition dipole (in units of debye^2) for the P- and R-branch transitions of the $02^{2e}0$–$01^{1e}0$ band of HCN. The solid line indicates the values calculated without any Herman–Wallis terms, but with the l-type resonance taken into account. The circles (O) indicate the measured values of $\mu^2 F$; see Eq. (1).

For the unperturbed transitions, $04^{2e}0$–$01^{1}0$, the Herman–Wallis terms given in Table III are in fair agreement with the value 0.00105 but more exact intensity calculations show that higher-order terms are needed to get better agreement.

The effect of l-type resonance is also important for determining the quadratic Herman–Wallis terms in many of the other transitions given in Tables III and IV, but when both the upper and lower states are involved in the l-type resonance, Watson's simple formula does not apply.

We have used an exact calculation of the l-type resonance interaction to obtain the intensities and effective Herman–Wallis constants for the Q-branch transitions for all the perpendicular transitions measured in this work. This calculation takes into account the mixing of the different states by using the eigenvectors from the l-type resonance calculation to determine the intensity of each transition. Trial fits of these calculated transition intensities to find effective Herman–Wallis constants shows that the fits are somewhat sensitive to the range of J-values used in the fits, as well as the maximum power of $J(J+1)$ used in the fit. As an example, when the calculated intensities for the $04^{2e}0$–$01^{1f}0$ transitions are fit to a Herman–Wallis function, Eq. (3), that involves only the A_2^Q term, the value of that term is 7.93×10^{-4} and the calculated intensities are only fit with two-digit accuracy, but when both the A_2^Q and A_4^Q terms are used then $A_2^Q = 10.7 \times 10^{-4}$ and all the calculated intensities are fit with four-digit accuracy.

In order to obtain a fair comparison between the calculated and measured Herman–Wallis constants, we used the calculated transition intensities for the same range of J-values as were measured and we fit them in the program used to fit the measured values. The values of A_2^Q determined from these calculated intensities are given in the last column of Table III for comparison with the measured values. The calculated transition intensities were not fit perfectly by the single Herman–Wallis constant, A_2^Q, and the uncertainties obtained from these fits of the calculated intensities reflect the need for adding higher-order effective Herman–Wallis terms.

Figure 3 gives a convincing demonstration of the accuracy of the l-type resonance calculation in matching the observed m-dependence of the intensity. In Fig. 3 the entire m-dependence shown by the solid curve is given by the l-type resonance and was calculated by the same program that gave the calculated A_2^Q values in the last column of Table III.

Some of the intensity measurements given in Table III involve transitions that begin in rather high energy levels even though all the measurements were made at room temperature. For the very highest energy levels in each set of measurements, the lines were very weak due to the unfavorable Boltzmann population factor and so in some cases only the Q-branch intensities were measured because they are generally twice as strong as the P- and R-branch lines. In those cases of high lower-state energy levels, the measured transitions only extended to $J = 12$ to 15, J-levels slightly above the intensity maximum. Consequently, the uncertainty in the Herman–Wallis constant is rather large.

Error Limits

The uncertainties given in Tables III and IV are the uncertainties given by the least-squares fit of the measured linestrengths and do not reflect any uncertainty in the temperature or in the pressure–path length product used in the analysis.

The temperature uncertainty will add an uncertainty of $\pm 0.5 \times 10^{-4}$ to the A_1^{PR} terms and an uncertainty of about $\pm 0.2 \times 10^{-4}$ to the other Herman–Wallis constants.

The temperature uncertainty will also add an uncertainty of about 2% to the transition dipoles for the hot bands originating from the $3\nu_2$ levels, about 1.2% to the transition dipoles for the hot bands originating from the $2\nu_2$ levels, and less than 1% to the uncertainties for the other transitions.

The pressure uncertainty does not affect the determination of the Herman–Wallis constants but dominates the uncertainty in the absolute values for the transition dipoles. The ratios of the hot-band transition dipoles to the ground state transition dipoles are probably accurate to within about 3%. In many cases that means that the measured change in the transition dipoles with lower state energy is not significant. The absolute uncertainties in the transition dipoles are quite large, about 10% in the best case and 20% for the 4800 cm^{-1} region.

DISCUSSION

By looking at a number of different hot bands illustrating most of the different cases possible through $\Delta v_2 = 4$, we have shown that Eqs. (6) and (7) are necessary for understanding the intensity of hot bands. If the L_2 term is left out of the analysis, the transition dipole of many hot bands would appear to be quite different from the ground state transition dipole. For example, the intensity of the 05^10–02^00 transitions would appear to be too great by a factor of 6 (compared to the intensity of transitions from the ground state, after correcting for the Boltzmann population) and the intensity of the 13^10–01^10 transitions would seem to be too great by a factor of 2.

The present measurements show that, when the L_2 term is included in the analysis, the transition dipole is only changed by a few percent in going from transitions from the ground state to transitions from other low lying vibrational states. Considering that most other rovibrational constants (such as B_v or ΔB_v) and even the dipole moment itself change by a few percent, such small changes in the transition dipole are not unexpected, provided strong resonances are absent.

For those bands that are not strongly affected by vibrational or Fermi resonances, the $L_{13}L_2$ terms are essential if one wishes to predict high temperature spectra from low temperature measurements. Such terms are also essential if one wishes to understand the changes in the transition dipole as a function of the lower state involved in a transition.

This work demonstrates the importance of l-type resonance in determining the Herman–Wallis effect. In the case of HCN, where vibrational resonances are weak enough to be ignored, both A_2^{PR} and A_2^{Q} are primarily determined by the effect of l-type resonance. Consequently, a program for calculating intensities of transitions that includes the effects of l-type resonance in the calculation will give very good agreement with the observed spectrum of HCN even if no additional Herman–Wallis contribution is included. This is easily seen in Fig. 3 where the calculated intensity matches the measured intensity even though no Herman–Wallis terms were used in the calculation of the intensity. However, the l-type resonance does not contribute significantly to the A_1^{PR} term which must come from other weak resonances.

APPENDIX A

This derivation of Eqs. (5)–(7) follows the notation and expressions used in Section 3-5 of Ref. (*22*), to which the reader should refer. If the electric dipole is expanded as a power series in the normal coordinates, one has

$$\mu = \mu_0 + \sum_n \mu_n Q_n + \sum_n \sum_m \mu_{nm} Q_n Q_m + \sum_n \sum_m \sum_l \mu_{nml} Q_n Q_m Q_l + \text{higher terms,} \quad \text{(A1)}$$

where μ is a vector quantity and $\mu_n = \partial\mu/\partial Q_n$, $\mu_{nm} = \partial^2\mu/\partial Q_n \partial Q_m$, etc. Now assume that the vibrational wave function ψ_v is a product of harmonic oscillator functions, then the intensity of a given absorption band is proportional to the square of

$$\int \psi_{v'}^* \mu \psi_{v''} d\tau_v = \mu_0 \int \psi_{v'}^* \psi_{v''} d\tau_v + \sum_n \mu_n \int \psi_{v'}^* Q_n \psi_{v''} d\tau_v + \sum_n \sum_m \mu_{nm} \int \psi_{v'}^* Q_n Q_m \psi_{v''} d\tau_v + \cdots \quad \text{(A2)}$$

The right-hand side of Eq. (A2) can be replaced by product wavefunctions in the normal coordinates for which the nonvanishing nondegenerate terms may be found in Appendix III of Ref. (*22*).

To evaluate the L_{13} term in Eq. (5), we only need to consider the nondegenerate vibrations. First we drop the term in μ_0, because it does not contribute to the infrared absorption, and if we only use the two nondegenerate vibrational fundamentals, ν_1 and ν_3, then Eq. (A2) becomes

$$\begin{aligned}
\int \psi_{v'}^* \mu \psi_{v''} d\tau_v = {} & \mu_1 \left[\prod_{i\neq 1} \int \psi_{v'}^*(Q_i)\psi_{v''}(Q_i)dQ_i\right] \int \psi_{v'}^*(Q_1)Q_1\psi_{v''}(Q_1)dQ_1 \\
& + \mu_3 \left[\prod_{i\neq 3} \int \psi_{v'}^*(Q_i)\psi_{v''}(Q_i)dQ_i\right] \int \psi_{v'}^*(Q_3)Q_3\psi_{v''}(Q_3)dQ_3 \\
& + \mu_{11} \left[\prod_{i\neq 1} \int \psi_{v'}^*(Q_i)\psi_{v''}(Q_i)dQ_i\right] \int \psi_{v'}^*(Q_1)Q_1^2\psi_{v''}(Q_1)dQ_1 \\
& + \mu_{13} \left[\prod_{i\neq 1,3} \int \psi_{v'}^*(Q_i)\psi_{v''}(Q_i)dQ_i\right] \int \psi_{v'}^*(Q_1)Q_1\psi_{v''}(Q_1)dQ_1 \\
& \times \int \psi_{v'}^*(Q_3)Q_3\psi_{v''}(Q_3)dQ_3 + \mu_{33} \left[\prod_{i\neq 3} \int \psi_{v'}^*(Q_i)\psi_{v''}(Q_i)dQ_i\right] \\
& \times \int \psi_{v'}^*(Q_3)Q_3^2\psi_{v''}(Q_3)dQ_3 + \text{higher terms.} \quad \text{(A3)}
\end{aligned}$$

If only the first nonvanishing term is considered, then the right-hand side of Eq. (A3) becomes proportional to

$$\begin{aligned}
(v_1 + 1)^{1/2}, &\qquad \text{for } v_1 \to v_1 + 1 \\
[(v_1 + 1)(v_1 + 2)]^{1/2}, &\qquad \text{for } v_1 \to v_1 + 2 \\
[(v_1 + 1)(v_1 + 2)(v_1 + 3)]^{1/2}, &\qquad \text{for } v_1 \to v_1 + 3 \\
&\text{etc.}
\end{aligned}$$

or

$$[(v_1 + \Delta v_1)!/v_1!]^{1/2}.$$

To normalize this term so that the factor is always 1 if $v_1 = 0$, it is necessary to divide by $\Delta v_1!$.

The intensity of a given transition is proportional to the square of Eq. (A2). Consequently, the ratio of the intensity of the hot-band transition from the vi-

brationally excited state, (v_1, v_3), to the intensity from the ground state will be given by

$$(v_1 + \Delta v_1)!(v_3 + \Delta v_3)!/(\Delta v_1! v_1! \Delta v_3! v_3!), \quad \text{(A4)}$$

which is the same as Eq. (5) given earlier. The extension to molecules with more nondegenerate vibrations is obvious.

The L_2 term, Eqs. (6) and (7), can be derived in the same way by making use of the equations for doubly degenerate modes, such as those given in the paper by Moffitt and Liehr (*23*). Alternatively, one can use ladder operators (sometimes called raising and lowering operators) for doubly degenerate vibrations (*24*).

The limitations of this approach are the assumption that the higher-order terms may be ignored and the assumption that a real vibrational state can be described by harmonic oscillator wavefunctions according to a unique vibrational assignment. In real life, each vibrational state will be a mixture of several vibrational states, even though one assignment can describe the major contribution to the true vibrational state. These limitations will probably become more important as one goes to the higher vibrational states or to higher hot bands.

ACKNOWLEDGMENTS

The authors thank John Johns (of the NRC of Canada) for allowing them to use the line-fitting program that he and others developed for the analysis of Fourier transform spectra. The help of G. Mellau in the experimental work at Giessen is gratefully acknowledged. Some intensity calculations were made by A. Loh. Two of the authors (A. M. and W. Q.) also thank Brenda and Manfred Winnewisser for their hospitality during visits to their laboratory while some of these measurements were being made. This project was possible with financial support of the Deutsche Forschungsgemeinschaft.

RECEIVED: December 7, 1994

REFERENCES

1. R. H. TIPPING, *J. Mol. Spectrosc.* **61,** 272–281 (1976).
2. N. LEGAY-SOMMAIRE AND F. LEGAY, *J. Mol. Spectrosc.* **8,** 1–8 (1962).
3. C. R. BRAZIER, N. H. OLIPHANT, AND P. F. BERNATH, *J. Mol. Spectrosc.* **134,** 421–432 (1989).
4. A. G. MAKI AND J. S. WELLS, "Wavenumber Calibration Tables From Heterodyne Frequency Measurements." NIST Special Publication 821, U.S. Government Printing Office, Washington, DC, 1991.
5. M. WEBER, W. B. BLASS, G. W. HALSEY, AND J. J. HILLMAN, *J. Mol. Spectrosc.* **165,** 107–123 (1994).
6. G. E. HYDE AND D. F. HORNIG, *J. Chem. Phys.* **20,** 647–652 (1952).
7. K. KIM AND W. T. KING, *J. Chem. Phys.* **71,** 1967–1972 (1979).
8. I. W. M. SMITH, *J. Chem. Soc. Faraday Trans. 2* **77,** 2357–2363 (1981).
9. W. QUAPP, S. KLEE, G. C. MELLAU, S. ALBERT, AND A. MAKI, *J. Mol. Spectrosc.* **167,** 375–382 (1994).
10. K. KEPPLER, Ph.D. dissertation, Ohio State University, Columbus, Ohio, 1995.
11. J. W. C. JOHNS AND J. VANDER AUWERA, *J. Mol. Spectrosc.* **140,** 71–102 (1990).
12. J. K. G. WATSON, *J. Mol. Spectrosc.* **125,** 428–441 (1987).
13. A. S. PINE, A. G. MAKI, AND N.-Y. CHOU, *J. Mol. Spectrosc.* **114,** 132–147 (1985).
14. J. W. C. JOHNS, *J. Mol. Spectrosc.* **125,** 442–464 (1987).
15. A. S. PINE AND J. P. LOONEY, *J. Chem. Phys.* **96,** 1704–1714 (1992).
16. H. S. PEISER, N. E. HOLDEN, P. DE BIEVE, I. L. BARNES, R. HAGEMANN, J. R. DELAETER, T. J. MURPHY, E. ROTH, M. SHIMA, AND H. G. THODE, *Pure Appl. Chem.* **56,** 696–768 (1984).
17. P. DE BIEVRE, M. GALLET, N. E. HOLDEN, AND I. L. BARNES, *J. Phys. Chem. Ref. Data* **13,** 809–891 (1984).
18. I. MILLS, T. CVITAŠ, K. HOMANN, N. KALLAY, AND K. KUCHITSU, "Quantities, Units and Symbols in Physical Chemistry, IUPAC," Blackwell Sci., Oxford, 1988.

19. R. S. McDowell, *J. Chem. Phys.* **88,** 356–361 (1988).
20. A. G. Maki, W. B. Olson, and R. L. Sams, *J. Mol. Spectrosc.* **36,** 433–447 (1970).
21. J. K. G. Watson, *J. Mol. Spectrosc.* **132,** 483–491 (1988).
22. E. B. Wilson, J. C. Decius, and P. C. Cross, "Molecular Vibrations—The Theory of Infrared and Raman Vibrational Spectra." McGraw–Hill, New York, 1955.
23. W. Moffitt and A. D. Liehr, *Phys. Rev.* **106,** 1195–1200 (1957).
24. H. W. Kroto, "Molecular Rotation Spectra." Dover, New York, 1992.